ACS OMEGA

http://pubs.acs.org/journal/acsodf

Article

Probing the Effect of Aliphatic Ionic Liquids on Asphaltene Aggregation Using Classical Molecular Dynamics Simulations

Surabhi Aswath, Poulumi Dey,* and Anoop Kishore Vatti*

Cite This: *ACS Omega* 2023, 8, 16186−16193

Read Online

ACCESS | Metrics & More | Article Recommendations | Supporting Information

ABSTRACT: One of the major constituents of heavy oil is asphaltenes. They are responsible for numerous problems in petroleum downstream and upstream processes, such as catalyst deactivation in heavy oil processing and blocking pipes while transporting crude oil. Probing the efficiency of new nonhazardous solvents in separating asphaltenes from crude oil is key to avoid conventional volatile and hazardous solvents by replacing these conventional solvents with new ones. In this work, we have investigated the efficiency of ionic liquids to separate asphaltenes from organic solvents (such as toluene and hexane) using molecular dynamics simulations. Triethylammonium-dihydrogen-phosphate and triethylammonium acetate ionic liquids are considered in this work. Various structural and dynamical properties are calculated, such as radial distribution function, end-to-end distance, trajectory density contour, and diffusivity of asphaltene in the ionic liquid-organic solvent mixture. Our results explain the role of anions, i.e., dihydrogen-phosphate and acetate ions, in separating asphaltene from toluene and hexane. Our study provides an important revelation about the dominant role played by the IL anion in intermolecular interactions which depends on the type of solvent (i.e., toluene or hexane) in which the asphaltene is present. The anion induces enhanced aggregation in the asphaltene-hexane mixture compared to the asphaltene-toluene mixture. The molecular insights obtained within this study on the role played by ionic liquid anion in asphaltene separation are key for the preparation of new ionic liquids for asphaltene precipitation applications.

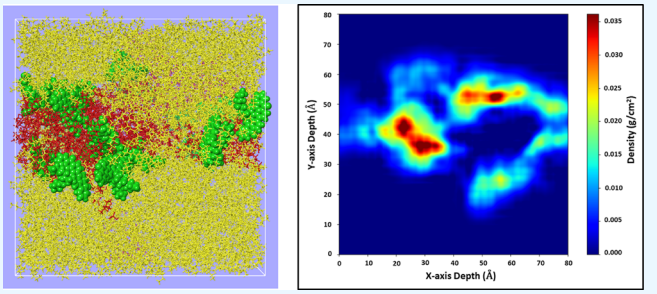

1. INTRODUCTION

Heavy crude oil and bitumen make up a majority of the world's total oil resources.[1] Their transportation and processing are challenging due to their low flowability.[2] The heavy crude oils are highly viscous and are primarily contaminated by heavy metals, sulfur and asphaltenes. Their high viscosity is attributed to the presence of asphaltenes,[3,4] whose precipitation is caused by changes in pressure, temperature, fluid properties, and contact with water or other organic solvents and solvents in which asphaltene is insoluble such as *n*-alkanes. Asphaltenes comprise alkyl side chains, metal and polar heteroatoms, and polyaromatic structures.[5] Some of the common ways to tackle the problem related to flowability of heavy crude oil are heating, blending with the light crude oil/diluent, etc. However, these approaches have their own challenges with respect to the cost and separation of the diluent from heavy crude oil.[6,7] The asphaltenes can be dissolved by treating them with nonpolar solvents, e.g., benzene or toluene; however, it is important to note that these solvents are hazardous and volatile. Lighter solvents, e.g., hexane or heptane, can be used, but they have lower solubility.[8,9]

Ionic liquids (ILs) are promising candidates and could be used to efficiently separate asphaltenes from crude oil[10−13] and can also separate bitumen from the oil sands.[14−16] ILs are environmental friendly and highly efficient organic salts because of the properties such as low melting point, good thermal and chemical stability, nonflammability, etc.[17,18] Addressing the issue of asphaltene separation using ILs can thus aid in the easy transportation of crude oil.

Pina et al.[19] discussed the characterization of asphaltenes in various solvents and evaluation of asphaltene flocculation point in solvents such as toluene, *p*-xylene, *m*-xylene, *o*-xylene, and ethylbenzene using heptane as a flocculant. The review elucidated several methods, including tonometry, ebulliometry, and size exclusion chromatography for determining molecular mass; viscosimetry, small angle scattering, and electron microscopy for colloidal structure; small angle neutron and X-ray scattering (SANS and SAXS) for studying asphaltene aggregates; and filter drop spreading and optical microscopy, light scattering, opacimetry, and nephelometry, among others, to visualize the extent of asphaltene flocculation. Painter et al.[14] conducted experimental investigations on the extraction of

Received: January 25, 2023
Accepted: April 3, 2023
Published: April 27, 2023

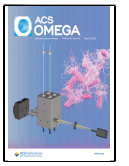

the bitumen from oil sands using the 1-butyl-2,3-dimethylimidazolium tetrafluoroborate ([bmmim][BF_4]) IL in combination with toluene solvent. In their work, 90% bitumen was recovered in successive extractions. Sakthivel et al.[10] performed experimental investigations using ultraviolet−visible (UV−vis) spectrophotometry, Fourier transform-infrared spectroscopy (FTIR), and ^{13}C-nuclear magnetic resonance (NMR) spectroscopy on the dissolution of asphaltene present in tank bottom sludge using nine aromatic ILs in different organic solvents such as decane, hexane, ethyl acetate, heptane, and toluene. It was shown in their work that the presence of ILs in organic solvents increases the efficiency of disaggregation by more than 50% as compared to the neat solvents. Sakthivel et al.[11] performed experimental studies using UV- visible, FTIR, and ^{13}C NMR spectroscopy to understand the dissolution of heavy crude oil using eight aliphatic ILs in various organic solvents. Their results showed a drastic increase in the dissolution percentage of heavy crude oil in the presence of the ILs as compared to neat solvents. Further, it was concluded that small quantity of IL is sufficient to achieve the complete dissolution of asphaltene. The [Et_3NH][H_2PO_4] IL showed superior performance compared to other ILs (such as [Et_3NH][BF_4],[Et_3NH][SO_4], [Bu_3NH][HSO_4] etc.) in the dissolution of crude oil in toluene, whereas [Et_3NH]-[CH_3COO] showed better performance in selected *n*-alkanes.

Subramanian et al.[20] experimentally investigated the flowability of the heavy and extra heavy crude oil on addition of the ILs. Further, the role of the IL alkyl tail length, counterion charge density, and cationic heads were investigated to reduce the viscosity of the Mexican heavy oil and Canadian and Venezuelan bitumen. The reduction of the viscosity is explained based on the molecular interactions between the ILs and the asphaltene molecules. Rashid et al.[21] investigated the role of the hydrophobic and hydrophilic ILs in the dispersion of the asphaltene aggregates using UV−visible spectroscopy. They found that hydrophobic ILs have more tendency to reduce the formation of asphaltene aggregates than the hydrophilic ones and can be considered as potential deflocculants. Atta et al.[22] prepared allyl imidazolium-based ILs using various organic anions such as oleate, cardanoxy, and abietate and employed them as asphaltene dispersants in Arabic heavy crude oil and heptane-toluene solvents. The IL-asphaltene interactions were quantified using zeta potential and size variations. The abietate-based IL showed the maximum asphaltene dispersion capability, followed by the oleate and cardanoxy-based ILs. The results of zeta potential highlighted the presence of positive surface charges in the abietate-based IL, which led to charge transfer and adsorption of the IL molecules on negatively charged asphaltenes. Thus, asphaltene aggregation was inhibited, with efficiencies reaching 90% in crude oil at IL concentrations of 0.15 g/L.

Headen et al.[23] conducted MD simulations of asphaltene aggregation using four asphaltene structures, including island, archipelago, and continental models, in two solvent environments, toluene and *n*-heptane. Additional systems incorporating resins and mixtures of different asphaltene structures were also simulated. The study reported the average cluster sizes, radii of gyration, densities, and relative shape anisotropies of the asphaltene clusters in each system. Three interesting observations of this study include the formation of predominantly spherical clusters as opposed to disk-shaped aggregates, the negligible role of resins as surfactants in asphaltene/toluene systems, and the occurrence of a continuous distribution of cluster sizes. Hernandez Bravo et al.[24] performed experimental investigation and molecular dynamics (MD) simulations of ILs and asphaltene. It was concluded that the IL-cation and asphaltene-π ligand molecular interactions are dominant between asphaltene-IL. Experimental viscosity measurement suggests that considered ILs can be potential candidates in the reduction of the viscosity of heavy crude oil. Ghamartale et al.[25] investigated the inhibitory effects of *n*-octylphenol on the aggregation of three different asphaltene structures based on the molecular weight in *n*-heptane using MD simulations. The number, size, shape, and density of the aggregates were calculated for each system. Octylphenol facilitated aromatic stacking and hydrogen bonds with the asphaltene molecules were observed for two asphaltene models. Asphaltene continued to aggregate over long simulation time scales, even in the presence of octyl phenol, indicating that the inhibitor only delayed the onset of aggregation. However, the performance of octylphenol greatly depended on the system's structure and heterogeneity of asphaltene.

EL-Hefnawy et al.[26] functionalized asphaltenes with carboxylic acid groups to incorporate them into functional imidazolium ILs by conjugating asphaltene carboxylate anions with 1,3-diheptyl (aliphatic - AsIL) and 1,3-diheptyl-2-hydroxyphenyl (aromatic - AHIL) imidazolium cations. The interactions between pure IL and asphaltenes in different compositions of toluene/heptane binary mixture were studied by dynamic light scattering (DLS) and zeta potential measurements to evaluate the dispersion of asphaltenes and charge transfer between the IL and asphaltene heteroatoms, respectively. The dispersion efficiency of AHIL was greater than that of AsIL, especially in an optimum IL and asphaltene ratio of 1:1. The interactions between the moieties in the IL and the asphaltene in crude oil prevented other unfavorable interactions which could lead to asphaltene aggregation. El Hoshoudy et al.[27] conducted experimental investigations and MD simulations to study the interactions between the imidazolium based ILs and the asphaltenes. The synthesized ILs were characterized using FTIR, ^{1}H NMR, Raman spectroscopy, and thermogravimetric (TGA) analysis.

Ghanem et al.[28] synthesized imidazolium based ILs and performed FTIR, ^{1}H NMR, TGA, and elemental analysis and also performed density functional theory (DFT) calculations to investigate the electronic properties of the ILs. The synthesized ILs showed good surface activity and thermal stability properties. It was concluded that with an increase in the alkyl chain length of the IL molecule, the asphaltene aggregation is promoted. Vatti et al.[13] performed experimental investigations and MD simulations of 1-butyl-3-methylimidazolium hexafluorophosphate IL and asphaltene. In their study, the role of IL in separating asphaltene from the toluene/hexane solvents was discussed. Further, $\pi-\pi$ stacking was observed between aromatic IL and asphaltene within this study. In recent study, Ghamartale et al.[29] conducted MD simulations to assess the changes in the aggregation of two continental asphaltene structures in *n*-heptane (7 wt % of asphaltene), in the presence and absence of three chemical inhibitors: octylphenol and two ILs, i.e., 1-butyl-3-methylimidazolium chloride ([BMIM][Cl]) and 1-butyl-3-methylimidazolium bromide ([BMIM][Br]). The study provided a detailed account of the mechanisms involved in asphaltene aggregation in the presence of ILs. Radial distribution function, aggregate shape (asphericity index), and angle distribution analyses were

https://doi.org/10.1021/acsomega.3c00515
ACS Omega 2023, 8, 16186−16193

Table 1. Number of Asphaltene, Toluene, Hexane and IL Molecules, i.e., $[Et_3NH]^+[CH_3COO]^-$ and $[Et_3NH]^+[H_2PO_4]^-$, along with the Simulation Box Sizes

mixture	asphaltene	toluene	hexane	IL	simulation box size (Å^3)
Asp+$[Et_3NH]^+[CH_3COO]^-$ + Toluene	24	2471	-	505	85.27 × 84.37 × 82.95
Asp+$[Et_3NH]^+[H_2PO_4]^-$ + Toluene	24	2554	-	422	84.27 × 82.82 × 83.15
Asp+$[Et_3NH]^+[CH_3COO]^-$ + Hexane	24	-	2495	481	86.38 × 90.27 × 90.91
Asp+$[Et_3NH]^+[H_2PO_4]^-$ + Hexane	24	-	2576	400	87.63 × 89.83 × 88.79

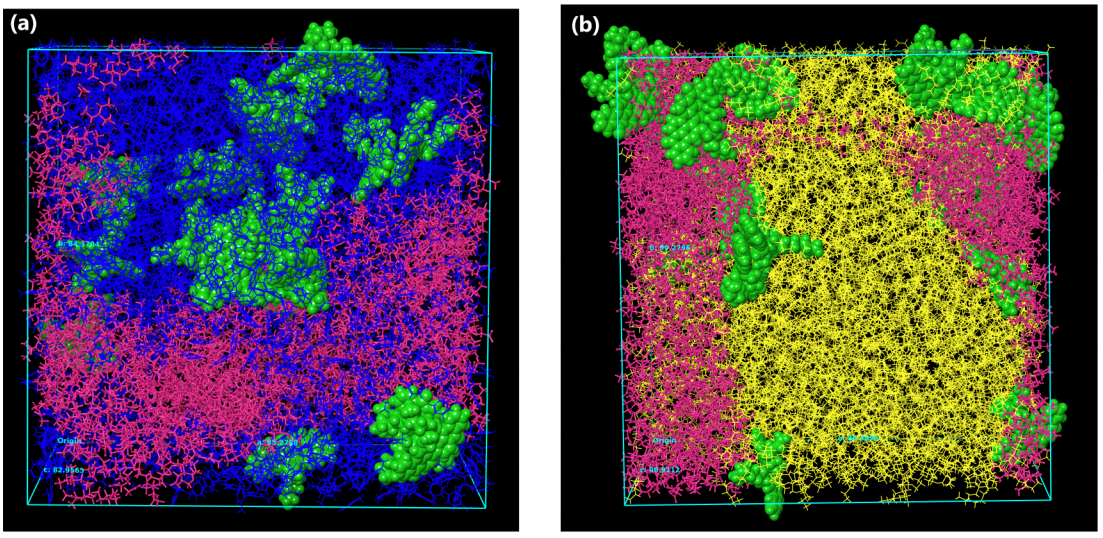

Figure 1. (a) Snapshot of the MD run of asphaltene aggregates in a toluene-$[Et_3NH]^+[CH_3COO]^-$ IL mixture. (b) Snapshot of the asphaltene aggregates in a hexane-$[Et_3NH]^+[CH_3COO]^-$ IL mixture. The pink color represents $[Et_3NH]^+[CH_3COO]^-$ IL, green represents asphaltene, blue represents toluene, and yellow represents hexane solvent molecules. The asphaltene molecules are seen in Corey Pauling Koltun (CPK) representation, and rest of the molecules are seen in a ball and stick representation.

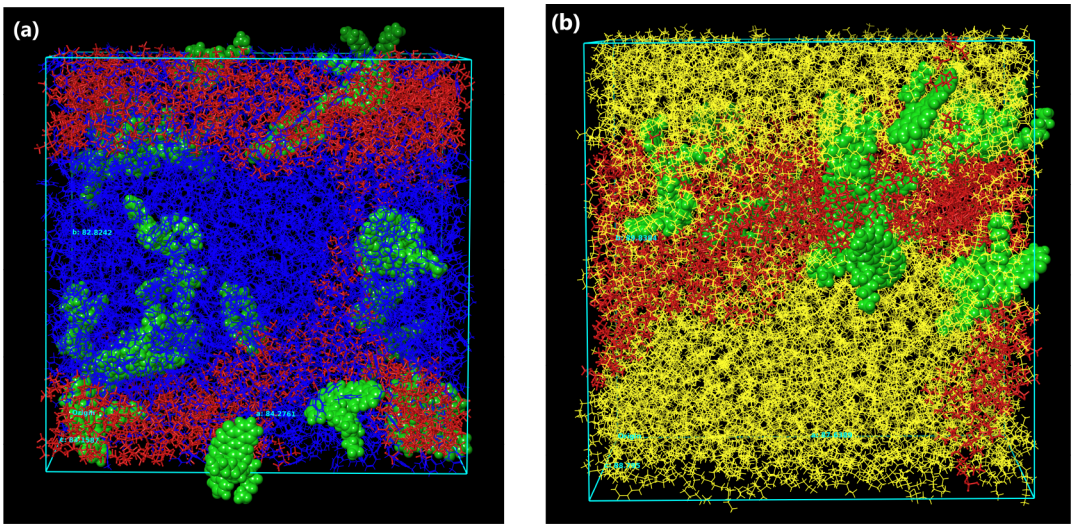

Figure 2. (a) Snapshot of the MD run of asphaltene aggregates in a toluene-$[Et_3NH]^+[H_2PO_4]^-$ IL mixture. (b) Snapshot of the asphaltene aggregates in a hexane-$[Et_3NH]^+[H_2PO_4]^-$ IL mixture. The red color represents $[Et_3NH]^+[H_2PO_4]^-$ IL, green represents asphaltene, blue represents toluene, and yellow represents hexane solvent molecules. The asphaltene molecules are visualized in a CPK model, and rest of the molecules are seen in a ball and stick model.

investigated to characterize the nature of clusters formed. [BMIM][Br] and [BMIM][Cl] hindered the formation of aggregates to a great extent due to the formation of strong cation−quadrupole interactions, which strongly competed against the quadrupole−quadrupole interactions of asphaltene cores.

The existing experimental works on asphaltene separation using ILs highlight several important aspects as elaborated above. However, molecular insights of interaction between IL anion and asphaltene based on the MD simulation technique are still lacking to the best of our knowledge. Within this study, a systematic analysis of the asphaltene aggregation using two ILs (i.e., $[Et_3NH]^+[CH_3COO]^-$ and $[Et_3NH]^+[H_2PO_4]^-$) in

https://doi.org/10.1021/acsomega.3c00515
ACS Omega 2023, 8, 16186−16193

Table 2. Persistence Length, Extended Chain Length, Molecular Standard Deviation, and the Time Series Mean of the End-to-End Distance of Asphaltene Molecules and Its Corresponding Standard Deviation over 80 ns of Production Run for Four Different Mixtures Considered in This Study

mixture	end-to-end distance (Å)	time series standard deviation (Å)	persistence length (Å)	extended chain length (Å)	molecular distribution standard deviation (Å)
Asp+$[Et_3NH]^+[CH_3COO]^-$ + Toluene	11.44	0.81	3.52	24.5	4.13
Asp+$[Et_3NH]^+[H_2PO_4]^-$ + Toluene	11.81	0.86	3.78	24.5	4.12
Asp+$[Et_3NH]^+[CH_3COO]^-$ + Hexane	11.27	0.81	3.37	24.5	3.96
Asp+$[Et_3NH]^+[H_2PO_4]^-$ + Hexane	11.48	0.75	3.52	24.5	3.97

toluene and hexane solvents are analyzed in depth. The role played by anions (i.e., $[CH_3COO]^-$ and $[H_2PO_4]^-$) in aggregation of asphaltene is explained in our work. We have analyzed the structural properties of asphaltene aggregates using radial distribution function (RDF) and end-to-end distance. Furthermore, we have reported the diffusion coefficient of asphaltene molecules in a IL-toluene/hexane mixture. Our results highlight the efficiency of the selected ILs in separation of the asphaltene from the toluene and hexane solvents. Our study made an important revelation about the dominant role played by the IL anion in intermolecular interactions for asphaltene in toluene and hexane; such a study is the first of its kind.

2. COMPUTATIONAL DETAILS

The molecular mass of asphaltene molecular compounds ranges from 500 to 1000 g/mol.[30] Further, 750 g/mol is considered the most probable molecular mass of the asphaltene.[31] Therefore, we have selected the asphaltene model compound ($(C_{50}H_{48}O_4)$ Violanthrone-79) with a molecular weight of 712.9 g/mol. The asphaltene molecule (Violanthrone-79), which contains nine aromatic rings, two linear aliphatic side groups, and four oxygen heteroatoms in the polyaromatic core, is considered within MD simulations. $[Et_3NH]^+[CH_3COO]^-$ IL, $[Et_3NH]^+[H_2PO_4]^-$ IL, toluene, and hexane explicit molecules are considered. Our simulations boxes account for 25 wt % of the IL and approximately 5 wt % of the asphaltene. Optimized Parameters for Liquid Simulations (OPLS4)[32] force fields are used to describe the bonded and nonbonded interactions. MD simulations are performed using the Desmond[33] package within Schrödinger simulation software.[34] A set of Lorentz−Berthelot mixing rules is used to determine the Lennard-Jones parameters. The time step of 2 fs is used to integrate the equation of motion. The simulation protocol of 20 ns NPT run is performed to get the equilibrated volume. Later, the production run of 80 ns is performed and then analyzed for property estimation. Throughout these simulations we have used 1 atm pressure and 300 K for the isobaric−isothermal (NPT) run and 300 K for the NVT run. The nonbonded interactions are truncated at 9 Å, and a Nose-Hoover thermostat is used. We have used the relaxation time of 2 ps for the Martyna-Tobias-Klein barostat and relaxation time of 1 ps for the Nose-Hoover thermostat. We have considered asphaltene in four mixtures as presented in Table 1. Snapshots of the aggregation of asphaltene molecules in toluene and hexane mixtures with $[Et_3NH]^+[CH_3COO]^-$ IL and $[Et_3NH]^+[H_2PO_4]^-$ IL are shown in Figures 1 and 2, respectively. In the presence of the IL, we observed dynamic heterogeneity for the asphaltene in a toluene-hexane mixture within the simulation box. The probable reason for this heterogeneity is the dynamics of the IL cations and anions being heterogeneous and depends on their interaction with the asphaltene and respective toluene/hexane solvent.

3. RESULTS AND DISCUSSION

3.1. End-to-End Distance. The end-to-end distance is calculated for the asphaltene molecules in an IL-toluene/hexane mixture. It is the distance between one end of the side chain to the other chain end. The end-to-end distance is an important parameter to assess asphaltene aggregation[13,35,36] and is calculated by considering the semiflexible side chains[37] within the worm-like chain model.[38] The end-to-end distance of the asphaltene molecule averaged over all asphaltene molecules is evaluated over the production run of MD using the following equation:[35−37,39]

$$\langle h^2 \rangle = 2L_P L_0[1 - (L_P/L_0)(1 - \exp(-L_0/L_P))] \quad (1)$$

where $\langle h^2 \rangle$ is the mean squared end-to-end distance, L_0 is the extended chain length, and L_P is the persistence length. The calculated end-to-end distances of asphaltene for four considered mixtures are summarized in Table 2. Figure 3a,b shows the end-to-end distance versus time and frequency versus end-to-end-distance for asphaltene in a toluene-$[Et_3NH]^+[CH_3COO]^-$ mixture, respectively. Further,the time series standard deviation of the mean end-to-end distance fit over an 80 ns time interval corresponding to Figure 3(a) is summarized in Table 2. Figure 3(b) shows a histogram of the mean end-to-end distances from the time series plot in the 80 ns time interval. The corresponding molecular distribution standard deviation of the mean end-to-end distance fit for the asphaltene is also presented in Table 2. The average end-to-end distance of 11.44 Å is observed for asphaltene, and the maximum frequency is found for 13.77 Å for asphaltene in a toluene-$[Et_3NH]^+[CH_3COO]^-$ mixture. The lowest end-to-end distance, i.e., 11.27 Å, is observed for the asphaltene in a $[Et_3NH]^+[CH_3COO]^-$-hexane mixture, which suggests the strong aggregation of the asphaltene molecules, whereas a slightly higher end-to-end distance is observed for the same IL in toluene solvent, i.e., 11.44 Å. Furthermore, the highest end-to-end distance is observed for a $[Et_3NH]^+[H_2PO_4]^-$-toluene solvent, suggesting that the aggregation is less pronounced for asphaltene in this particular mixture. Overall, both the ILs have been found to have a superior performance in enhancing the aggregation in hexane solvent as compared to the toluene solvent.

3.2. Radial Distribution Function. Classical MD simulations have been extensively used to study the structural properties of liquids. We have calculated radial distribution

https://doi.org/10.1021/acsomega.3c00515
ACS Omega 2023, 8, 16186−16193

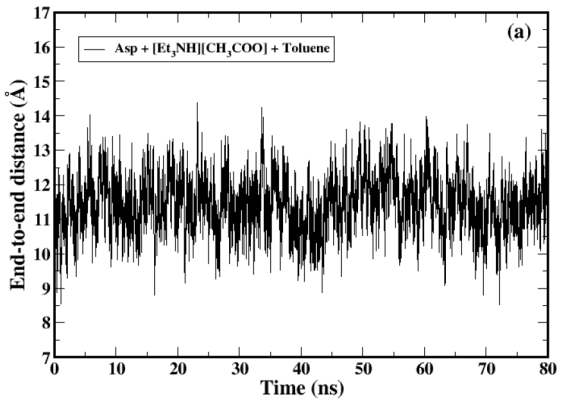

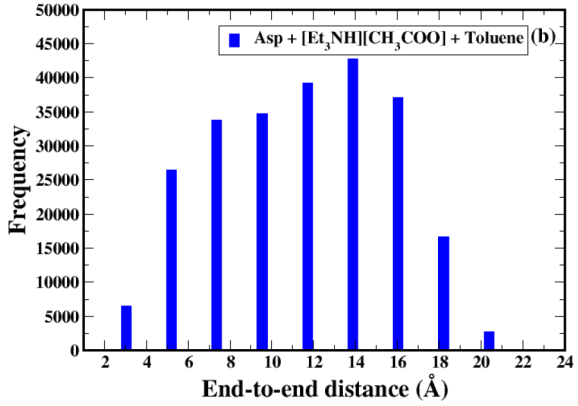

Figure 3. (a) The end-to-end distance of asphaltene molecules versus time in a toluene-$[Et_3NH]^+[CH_3COO]^-$ mixture. (b) Frequency vs end-to-end distance of asphaltene in a toluene-$[Et_3NH]^+[CH_3COO]^-$ mixture.

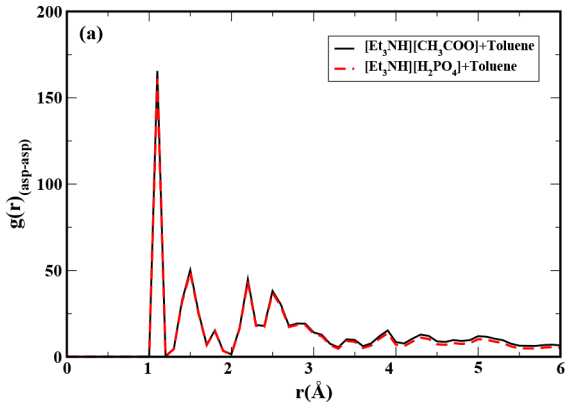

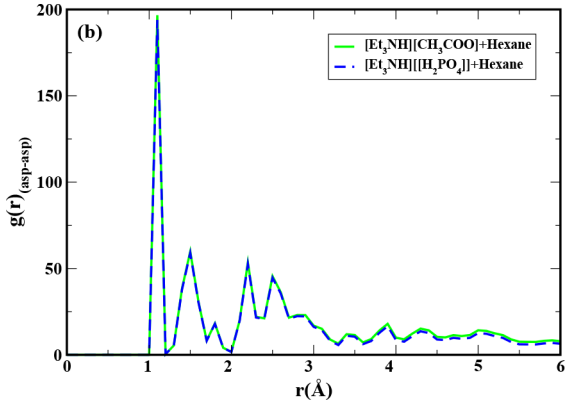

Figure 4. Radial distribution function of asphaltene-asphaltene pair in (a) $[Et_3NH]^+[CH_3COO]^-$ and $[Et_3NH]^+[H_2PO_4]^-$ in toluene (b) $[Et_3NH]^+[CH_3COO]^-$ and $[Et_3NH]^+[H_2PO_4]^-$ in hexane.

function (RDF) to explore the average distribution of the aggregates in the solvent mixture. The analysis of the aggregates is performed by RDF calculations as shown in Figure 4. RDF between the asphaltene-asphaltene pair indicates the probability that the asphaltene molecule is at a distance "r" from another asphaltene molecule. The asphaltene−asphaltene pair is selected to quantify the aggregation in different IL-toluene/hexane mixtures. Figure 4(a,b) shows the RDF between asphaltene-asphaltene pair in $[Et_3NH]^+[CH_3COO]^-$ and $[Et_3NH]^+[H_2PO_4]^-$ in toluene and $[Et_3NH]^+[CH_3COO]^-$ and $[Et_3NH]^+[H_2PO_4]^-$ in hexane, respectively. We observed asphaltene aggregates in the presence of the IL in both toluene and hexane mixtures. In the presence of the IL, it is interesting to note that the asphaltene aggregates are more in hexane than in toluene. We noticed that the probability, i.e., $g(r)_{(asp-asp)}$ is higher for the IL in hexane solvent than in toluene as shown in Figure 4. In case of both ILs, we observed peaks at 1.15, 1.5, and 2.2 Å. The first peak represents the aggregation of asphaltene molecules due to $\pi-\pi$ stacking, and the second peak represents their other stacking arrangement (Figure S1 of the Supporting Information), e.g., T-shape stacking as observed in an earlier work.[40] The third peak shows how strong the ordering of the asphaltene is in the respective mixture.

3.3. Diffusion Coefficient. The diffusivity of the asphaltene molecules is evaluated by calculating the slope of the mean-square displacement as a function of time as shown

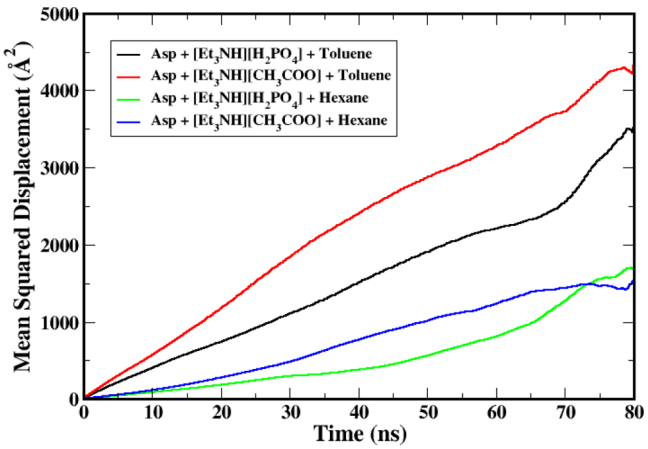

Figure 5. Mean squared displacement of asphaltene in four different asphaltene-IL-toluene/hexane mixtures.

in Figure 5 using the Einstein relation:[41] where $\langle|\vec{r}(t) - \vec{r}(0)|^2\rangle$ is the mean-square displacement. The calculated diffusion coefficients are presented in Table 3 for the considered mixtures of asphaltene. It is evident from Figure 5 that mean square displacement changes linearly with time, and therefore the diffusion coefficient of asphaltene can be

https://doi.org/10.1021/acsomega.3c00515
ACS Omega 2023, 8, 16186−16193

Table 3. Obtained Diffusion Coefficients (in m^2/s) of Asphaltene in the Presence of IL in Toluene and Hexane along with the Standard Deviation (σ)[a]

concentration	diffusion coefficient (m^2/s)	σ (m^2/s)	R^2
Asp+$[Et_3NH]^+[CH_3COO]^-$ + Toluene	8.92×10^{-11}	6.58×10^{-14}	0.994
Asp+$[Et_3NH]^+[H_2PO_4]^-$ + Toluene	5.22×10^{-11}	4.98×10^{-14}	0.985
Asp+$[Et_3NH]^+[CH_3COO]^-$ + Hexane	3.71×10^{-11}	3.45×10^{-14}	0.988
Asp+$[Et_3NH]^+[H_2PO_4]^-$ + Hexane	1.90×10^{-11}	3.97×10^{-14}	0.883

[a]R^2 of the fit is also shown.

modeled by the Einstein relation. The diffusion coefficient of the asphaltene is highest, i.e., 8.92×10^{-11} m^2/s in $[Et_3NH]^+[CH_3COO]^-$-toluene. It is evident that $[CH_3COO]^-$ based IL induces less aggregation in a toluene mixture in comparison to the $[H_2PO_4]^-$ based IL in toluene as the diffusivity of asphaltene is lower, i.e., 5.22×10^{-11} m^2/s for the latter case. Furthermore, the diffusion coefficient of the asphaltene is lowest, i.e., 1.90×10^{-11} m^2/s in a $[Et_3NH]^+[H_2PO_4]^-$-hexane mixture. It can thus be concluded from this study that $[H_2PO_4]^-$ IL induces stronger aggregation in a hexane mixture in comparison to $[Et_3NH]^+[CH_3COO]^-$ IL in hexane as the diffusivity of asphaltene is higher, i.e., 3.71×10^{-11} m^2/s, for the latter case. This observation can be explained by the restricted motion of asphaltene molecules owing to the formation of few aggregates in a $[H_2PO_4]^-$ IL-hexane mixture, which is supported by the density contours analysis presented in the following section.

$$D = \frac{1}{6}\lim_{t\to\infty}\frac{d}{dt}\langle|\vec{r}(t) - \vec{r}(0)|^2\rangle \quad (2)$$

3.4. Density Contour Analysis. The density profile and the cross sections are calculated by taking layers of a specified thickness perpendicular to the *XY*-Cartesian coordinate axis. To calculate the density profile at a particular point on the axis (defined as the coordinate at the bottom of the layer), the fraction of the van der Waals volume of each atom that overlaps the layer is multiplied by its atomic mass, and the result is summed over all specified atoms, then divided by the volume of the layer. Likewise, for the cross section, the layer is partitioned into cubes, and the volume fraction of each atom that overlaps each cube is determined and weighted by the atomic mass, summed and divided by the cube volume to give the density in the cube.

It is interesting to note that the acetate ion induces aggregation of the asphaltene in both toluene and hexane as can be seen in Figure 6 where the aggregates are shown in red color. It can be seen from the figure that the intensity is more for hexane solvent as compared to toluene solvent. The asphaltenes are insoluble in the hexane, and further the presence of IL enhances the asphaltene aggregation. Figure 7 shows that the $[H_2PO_4]^-$ ion based IL induces aggregation of the asphaltene in both toluene and hexane. The $[H_2PO_4]^-$ induced aggregates are observed to be more pronounced in the hexane solvent than in toluene. To conclude this study, both the selected ILs have a tendency to aggregate asphaltene in toluene and hexane, but stronger aggregation is noticed in the case of a IL-hexane mixture.

4. CONCLUSIONS

ILs have shown great potential to handle the environmental and energy challenges and further facilitate transportation of heavy crude oil. In this study, we investigated the effect of IL anions on asphaltene aggregation in toluene/hexane solvents using MD simulations. The role played by $[CH_3COO]^-$ and $[H_2PO_4]^-$ anions based ILs in asphaltene aggregation is understood by probing the structural and dynamic properties of the mixtures. The lowest end-to-end distance of asphaltene is observed for the $[CH_3COO]^-$ based IL in hexane solvent. The radial distribution function of the asphaltene−asphaltene pair suggests that there is $\pi-\pi$ stacking within the asphaltene aggregates. Furthermore, the lowest diffusion coefficient is observed for asphaltene in a $[Et_3NH]^+[H_2PO_4]^-$ IL-hexane mixture owing to the formation of few aggregates. Last but not the least, it is confirmed from the density contour analysis that $[H_2PO_4]^-$ based IL induces stronger aggregation in hexane than in toluene. To summarize our study, it is observed that both the selected ILs have a tendency to aggregate asphaltene in both toluene and hexane where stronger aggregation is noticed in the case of a IL-hexane mixture. It is important to take into account the impact of the type of IL anion on the synthesis of ILs, especially for the applications involving

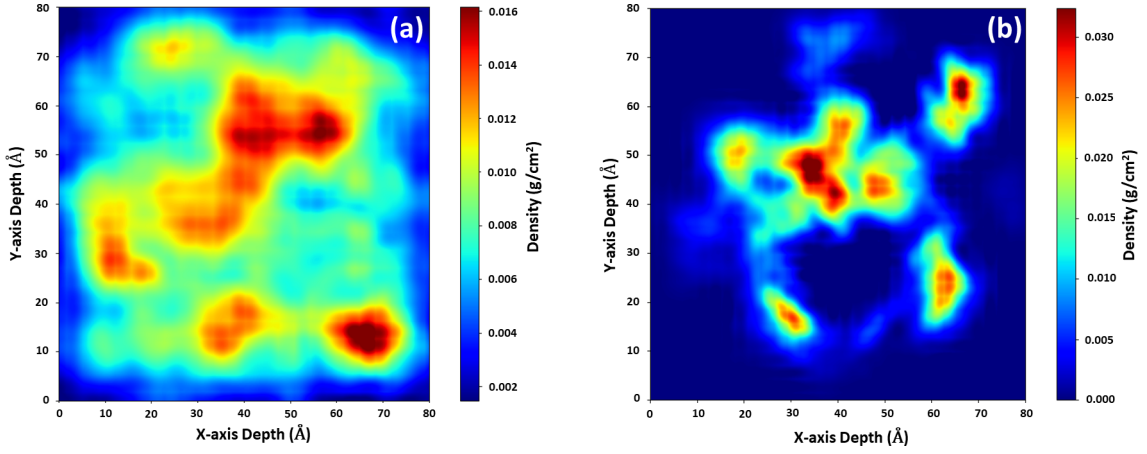

Figure 6. Trajectory density contours for (a) asphaltene in a toluene-$[Et_3NH]^+[CH_3COO]^-$ mixture. (b) Asphaltene in a hexane-$[Et_3NH]^+[CH_3COO]^-$ mixture.

https://doi.org/10.1021/acsomega.3c00515
ACS Omega 2023, 8, 16186−16193

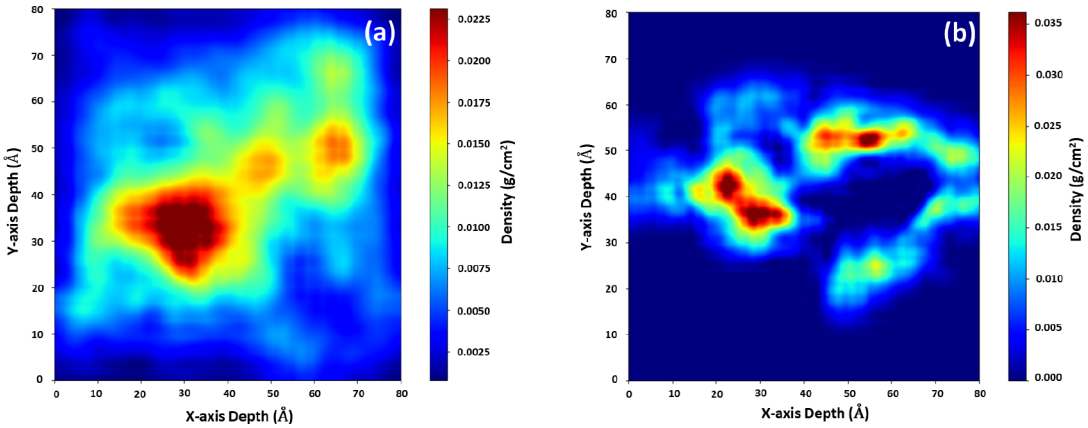

Figure 7. Trajectory density contours for (a) asphaltene in a toluene-$[Et_3NH]^+[H_2PO_4]^-$ mixture. (b) Asphaltene in a hexane-$[Et_3NH]^+[H_2PO_4]^-$ mixture.

asphaltene precipitation, which will allow replacing the conventional hazardous solvents with ILs.

■ ASSOCIATED CONTENT

Supporting Information

The Supporting Information is available free of charge at https://pubs.acs.org/doi/10.1021/acsomega.3c00515.

The atomistic structure snapshot of the single representative aggregate of the asphaltene (PDF)

■ AUTHOR INFORMATION

Corresponding Authors

Poulumi Dey − *Department of Materials Science and Engineering, Faculty of Mechanical, Maritime and Materials Engineering (3mE), Delft University of Technology, 2628 CD Delft, The Netherlands;* orcid.org/0000-0003-4679-1752; Email: P.Dey@tudelft.nl

Anoop Kishore Vatti − *Department of Chemical Engineering, Manipal Institute of Technology (MIT), Manipal Academy of Higher Education (MAHE), Manipal 576104 Karnataka, India;* orcid.org/0000-0003-3023-3684; Email: anoop.vatti@manipal.edu

Author

Surabhi Aswath − *Department of Chemical Engineering, Manipal Institute of Technology (MIT), Manipal Academy of Higher Education (MAHE), Manipal 576104 Karnataka, India;* orcid.org/0000-0003-0117-8444

Complete contact information is available at: https://pubs.acs.org/10.1021/acsomega.3c00515

Notes

The authors declare no competing financial interest.

■ ACKNOWLEDGMENTS

Anoop Kishore Vatti would like to thank the Schrödinger Centre for Molecular Simulations, MAHE, Manipal for their support.

■ REFERENCES

(1) Zhang, H.-Q.; Sarica, C.; Pereyra, E. Review of high-viscosity oil multiphase pipe flow. *Energy Fuels* **2012**, *26*, 3979−3985.

(2) Saniere, A.; Henaut, I.; Argillier, J. Pipeline transportation of heavy oils, a strategic, economic and technological challenge. *Oil and gas science and technology* **2004**, *59*, 455−466.

(3) Ilyin, S.; Arinina, M.; Polyakova, M.; Bondarenko, G.; Konstantinov, I.; Kulichikhin, V.; Malkin, A. Asphaltenes in heavy crude oil: Designation, precipitation, solutions, and effects on viscosity. *J. Pet. Sci. Eng.* **2016**, *147*, 211−217.

(4) Rashid, Z.; Wilfred, C. D.; Gnanasundaram, N.; Arunagiri, A.; Murugesan, T. A comprehensive review on the recent advances on the petroleum asphaltene aggregation. *J. Pet. Sci. Eng.* **2019**, *176*, 249−268.

(5) Spiecker, P.; Gawrys, K. L.; Kilpatrick, P. K. Aggregation and solubility behavior of asphaltenes and their subfractions. *J. Colloid Interface Sci.* **2003**, *267*, 178−193.

(6) Yaghi, B. M.; Al-Bemani, A. Heavy crude oil viscosity reduction for pipeline transportation. *Energy sources* **2002**, *24*, 93−102.

(7) Mustaffa, N. B. M. Oil pipeline wax deposition inhibition using chemical methods; B. Tech. Thesis, University Malaysia Pahang, Pahang, Malaysia, 2010.

(8) De Boer, R.; Leerlooyer, K.; Eigner, M.; Van Bergen, A. Screening of crude oils for asphalt precipitation: theory, practice, and the selection of inhibitors. *SPE Production & Facilities* **1995**, *10*, 55−61.

(9) Hart, A. A review of technologies for transporting heavy crude oil and bitumen via pipelines. *Journal of Petroleum Exploration and Production Technology* **2014**, *4*, 327−336.

(10) Sakthivel, S.; Velusamy, S.; Gardas, R. L.; Sangwai, J. S. Eco-efficient and green method for the enhanced dissolution of aromatic crude oil sludge using ionic liquids. *RSC Adv.* **2014**, *4*, 31007−31018.

(11) Sakthivel, S.; Velusamy, S.; Gardas, R. L.; Sangwai, J. S. Experimental investigation on the effect of aliphatic ionic liquids on the solubility of heavy crude oil using UV−visible, Fourier transform-infrared, and 13C NMR spectroscopy. *Energy Fuels* **2014**, *28*, 6151−6162.

(12) Sakthivel, S.; Velusamy, S. Effect of ammonium based ionic liquids on the rheological behavior of the heavy crude oil for high pressure and high temperature conditions. *Petroleum* **2022**, *8*, 552−566.

(13) Vatti, A. K.; Dey, P.; Acharya, S.; Kundarapu, L. K.; Puttapati, S. K. Role of Ionic Liquid in Asphaltene Dissolution: A Combined Experimental and Molecular Dynamics Study. *Energy Fuels* **2022**, *36*, 9111−9120.

(14) Painter, P.; Williams, P.; Lupinsky, A. Recovery of Bitumen from Utah Tar Sands Using Ionic Liquids. *Energy Fuels* **2010**, *24*, 5081−5088.

(15) Li, X.; Sun, W.; Wu, G.; He, L.; Li, H.; Sui, H. Ionic Liquid Enhanced Solvent Extraction for Bitumen Recovery from Oil Sands. *Energy Fuels* **2011**, *25*, 5224−5231.

(16) Berton, P.; Manouchehr, S.; Wong, K.; Ahmadi, Z.; Abdelfatah, E.; Rogers, R. D.; Bryant, S. L. Ionic Liquids-Based Bitumen Extraction: Enabling Recovery with Environmental Footprint Comparable to Conventional Oil. *ACS Sustainable Chem. Eng.* **2020**, *8*, 632−641.
(17) Welton, T. Room-temperature ionic liquids. Solvents for synthesis and catalysis. *Chem. Rev.* **1999**, *99*, 2071−2084.
(18) Kohno, Y.; Ohno, H. Ionic liquid/water mixtures: from hostility to conciliation. *Chem. Commun.* **2012**, *48*, 7119−7130.
(19) Pina, A.; Mougin, P.; Behar, E. Characterisation of Asphaltenes and Modelling of Flocculation - State of the Art. *Oil & Gas Science and Technology - Revue de lIFP* **2006**, *61*, 319−343.
(20) Subramanian, D.; Wu, K.; Firoozabadi, A. Ionic liquids as viscosity modifiers for heavy and extra-heavy crude oils. *Fuel* **2015**, *143*, 519−526.
(21) Rashid, Z.; Wilfredand, C. D.; Murugesan, T. *AIP Conference Proceedings*; 2017; Vol. *1891*; p 020118.
(22) Atta, A. M.; Ezzat, A. O.; Abdullah, M. M.; Hashem, A. I. Effect of Different Families of Hydrophobic Anions of Imadazolium Ionic Liquids on Asphaltene Dispersants in Heavy Crude Oil. *Energy Fuels* **2017**, *31*, 8045−8053.
(23) Headen, T. F.; Boek, E. S.; Jackson, G.; Totton, T. S.; Müller, E. A. Simulation of Asphaltene Aggregation through Molecular Dynamics: Insights and Limitations. *Energy Fuels* **2017**, *31*, 1108−1125.
(24) Hernandez Bravo, R.; Miranda, A.; Martinez-Magadan, J.-M.; Dominguez, J. Experimental and Theoretical Study on Supramolecular Ionic Liquid (IL)−Asphaltene Complex Interactions and Their Effects on the Flow Properties of Heavy Crude Oils. *J. Phys. Chem. B* **2018**, *122*, 4325−4335.
(25) Ghamartale, A.; Zendehboudi, S.; Rezaei, N. New Molecular Insights into Aggregation of Pure and Mixed Asphaltenes in the Presence of n-Octylphenol Inhibitor. *Energy Fuels* **2020**, *34*, 13186−13207.
(26) EL-Hefnawy, M. E.; Atta, A. M.; El-Newehy, M.; Ismail, A. I. Synthesis and characterization of imidazolium asphaltenes poly (ionic liquid) and application in asphaltene aggregation inhibition of heavy crude oil. *Journal of Materials Research and Technology* **2020**, *9*, 14682−14694.
(27) El Hoshoudy, A.; Ghanem, A.; Desouky, S. Imidazolium-based ionic liquids for asphaltene dispersion; experimental and computational studies. *J. Mol. Liq.* **2021**, *324*, 114698.
(28) Ghanem, A.; Alharthy, R. D.; Desouky, S. M.; El-Nagar, R. A. Synthesis and Characterization of Imidazolium-Based Ionic Liquids and Evaluating Their Performance as Asphaltene Dispersants. *Materials* **2022**, *15*, 1600.
(29) Ghamartale, A.; Rezaei, N.; Zendehboudi, S. Alternation of asphaltene binding arrangement in the presence of chemical inhibitors: Molecular dynamics simulation strategy. *Fuel* **2023**, *336*, 127001.
(30) Groenzin, H.; Mullins, O. C. Asphaltene Molecular Size and Structure. *J. Phys. Chem. A* **1999**, *103*, 11237−11245.
(31) Mullins, O. C.; et al. Advances in Asphaltene Science and the Yen-Mullins Model. *Energy Fuels* **2012**, *26*, 3986−4003.
(32) Lu, C.; Wu, C.; Ghoreishi, D.; Chen, W.; Wang, L.; Damm, W.; Ross, G. A.; Dahlgren, M. K.; Russell, E.; Von Bargen, C. D.; Abel, R.; Friesner, R. A.; Harder, E. D. OPLS4: Improving Force Field Accuracy on Challenging Regimes of Chemical Space. *J. Chem. Theory Comput.* **2021**, *17*, 4291−4300. PMID: 34096718
(33) Bowers, K. J.; Chow, E.; Xu, H.; Dror, R. O.; Eastwood, M. P.; Gregersen, B. A.; Klepeis, J. L.; Kolossvary, I.; Moraes, M. A.; Sacerdoti, F. D.; Salmon, J. K.; Shan, Y.; Shaw, D. E. *Proceedings of the 2006 ACM/IEEE Conference on Supercomputing; SC '06*; ACM: New York, NY, USA, 2006.
(34) *Schrödinger, Schrödinger* 2021-1; Schrödinger, LLC: New York, NY, 2021.
(35) Vatti, A. K.; Caratsch, A.; Sarkar, S.; Kundarapu, L. K.; Gadag, S.; Nayak, U. Y.; Dey, P. Asphaltene Aggregation in Aqueous Solution Using Different Water Models: A Classical Molecular Dynamics Study. *ACS Omega* **2020**, *5*, 16530−16536.
(36) Kundarapu, L. K.; Choudhury, S.; Acharya, S.; Vatti, A. K.; Pandiyan, S.; Gadag, S.; Nayak, U. Y.; Dey, P. Combined experimental and molecular dynamics investigation of 1D rod-like asphaltene aggregation in toluene-hexane mixture. *J. Mol. Liq.* **2021**, *339*, 116812.
(37) Brinkers, S.; Dietrich, H. R. C.; de Groote, F. H.; Young, I. T.; Rieger, B. The persistence length of double stranded DNA determined using dark field tethered particle motion. *J. Chem. Phys.* **2009**, *130*, 215105.
(38) Milstein, J. N.; Meiners, J.-C. In *Encyclopedia of Biophysics*; Roberts, G. C. K., Ed.; Springer Berlin Heidelberg: Berlin, Heidelberg, 2013; pp 2757−2760.
(39) Zhang, J.-Z.; Peng, X.-Y.; Liu, S.; Jiang, B.-P.; Ji, S.-C.; Shen, X.-C. The Persistence Length of Semiflexible Polymers in Lattice Monte Carlo Simulations. *Polymers* **2019**, *11*, 295.
(40) Khalaf, M. H.; Mansoori, G. A. A new insight into asphaltenes aggregation onset at molecular level in crude oil (an MD simulation study). *J. Pet. Sci. Eng.* **2018**, *162*, 244−250.
(41) Frenkel, D., Smit, B., Eds. *Understanding Molecular Simulation*, 2nd ed.; Academic Press: San Diego, 2002.

https://doi.org/10.1021/acsomega.3c00515
ACS Omega 2023, 8, 16186−16193